European Journal of Pharmaceutics and Biopharmaceutics 191 (2023) 235–246

Contents lists available at ScienceDirect

European Journal of Pharmaceutics and Biopharmaceutics

journal homepage: www.elsevier.com/locate/ejpb

Research paper

Design, development and *in vitro* quantification of novel electrosprayed everolimus-loaded Soluplus®/Polyvinyl alcohol nanoparticles via stability-indicating HPLC method in cancer therapy

Lynn Louis [a], Bor Shin Chee [a], Marion McAfee [b], Michael J.D. Nugent [a,*]

[a] PRISM Research Institute, Technological University of the Shannon, Athlone, Co. Westmeath, Ireland
[b] Centre for Mathematical Modelling and Intelligent Systems for Health and Environment (MISHE), Atlantic Technological University, Sligo, Ireland

ARTICLE INFO

Keywords:
RAD001
High-Performance Liquid Chromatography
Cross-linking
Freeze-thawing
Forced Degradation
Sustained Release
Bioavailability

ABSTRACT

Everolimus (RAD001) a mammalian target of rapamycin has been hampered by poor solubility, affecting its dissolution rate, a relationship that extends to low bioavailability. Nanoparticles (NP) based on Soluplus (SOL®) and Polyvinyl alcohol (PVA) was fabricated by electrospraying (ES) for the delivery of RAD001 to improve anti-tumour efficacy. Electrospraying with established experimental conditions produced PVA-SOL®-RAD001 NP with 71 nm mean diameter, smaller particle size distribution and >90 % encapsulation efficiency. Various polymer-drug concentrations exposed to various freeze–thaw (F/T) cycles were studied for NP optimisation and to enhance its mechanical properties. The optimised NP formulation demonstrated complete encapsulation as well as a sustained and pH dependent drug release profile for *in vitro* release test. In addition, to specifically study the degradation profile of RAD001 and to quantify RAD001 in the fabricated NP, a new HPLC method was developed and validated. The purpose and novelty of the HPLC method was also to ensure that RAD001 can be detected at low amounts where other conventional characterisation methods are unable to detect. The developed HPLC method was accurate, precise, robust and sensitive with LOD and LOQ values of 4.149 and 12.575 μg/mL. In conclusion, the novel developed HPLC system can be applied for the quantification of different chemotherapeutic agents and the novel electrosprayed hydrogel NP is a potential drug delivery system to increase solubility and bioavailability of RAD001 in cancer therapy.

1. Introduction

RAD001 is a potent macrolide analog of Sirolimus, made up of a 31 membered macrolide lactone [1,2]. The role of RAD001 is to inhibit mTOR activity rendering it an immunosuppressant with anti-proliferative activity [3]. The chemical structure of RAD001 consists of 40-O-[2-Hydroxyethyl] with a chemical formula of $C_{53}H_{83}NO_{14}$. RAD001 has been widely used as a chemotherapeutic agent in oncology as well as treating benign tumours such as subependymal giant cell astrocytoma (SEGA) secondary to tuberous sclerosis complex [4,5]. Despite RAD001 showing promising results in brain tumour treatment, the high dose mediated cytotoxity and low bioavailability hamper its clinical application. RAD001 is also reported to be unstable in gastric acid and its oral bioavailability is limited to 14 % in paediatric oncology [6,7]. Therefore, high doses of RAD001 are required orally to achieve the desired pharmacodynamic response, resulting in severe side effects associated with therapy which includes hypertriglyceridaemia, hypercholesterolaemia, opportunistic infections, thrombocytopenia and leukocytopenia [6]. As a consequence, routine performance of therapeutic drug monitoring is required to analyse the cumulative effect of RAD001 in treating patients with SEGA due to frequent dosing. Therefore, the need for a sustained release cannot be overemphasized to circumvent the high dose requirement of RAD001. In the treatment of brain tumours, a sustained release is a desired characteristic whereby it may lead to enhanced drug accumulation in the tumour region a relationship that extends to a reduction in dosing frequency required to exert a therapeutic response.

In our previously reported work, we developed a PVA microsphere embedded with RAD001 aiming to treat a benign tumour known as subependymal giant cell astrocytoma (SEGA) [4] by increasing solubility of RAD001 and to achieve a sustained release. In this paper, electrospraying was employed to reduce the size of the particles to nanoscale in

* Corresponding author.
E-mail address: Michael.Nugent@tus.ie (M.J.D. Nugent).

https://doi.org/10.1016/j.ejpb.2023.09.008
Received 24 June 2023; Received in revised form 21 August 2023; Accepted 12 September 2023
Available online 14 September 2023

comparison to the previously employed sessile droplet technique. (See Fig. 1.)

To the best of our knowledge, RAD001 has never been fabricated via the electospraying (ES) technique. ES is a promising technique and an innovative alternative to electrospinning that has proven its ability to form microparticles as well as NP in the development of a drug delivery system. The formation of micro- or NP is governed by the charged droplets theory whereby an electric field is passed through the charged liquid droplet which is composed of the Active Pharmaceutical Ingredients (API) and inert polymer via a nozzle deforming the liquid interface subsequently forming a Taylor cone [9,10]. At the tip of the cone, the free surface charges are accumulated, leading to a jet formation, which then breaks into droplets. The high voltage applied to this charged liquid causes an electrostatic force which helps to overcome the surface tension of the droplet known as the Rayleigh limit forming micro- or NP [11]. Compared to our previous work on PVA microspheres via the sessile droplet technique, electrospinning is employed here due to its advantages such as better encapsulation efficiency, higher loading efficiency, narrow particle size distribution and ease of synthesis due to it being a one step process [9–12].

In this study, the rationale behind the selection of SOL® (polyvinyl caprolactam–polyvinyl acetate–polyethylene glycol graft copolymer) a novel amphiphilic graft copolymer in the form of an amorphous solid dispersion in combination with PVA a hydrophilic polymer is to ensure that RAD001 is completely converted from a crystalline to an amorphous state when blended with the two polymers to achieve a sustained release [4]. The limitation of a solid dispersion however is, when a drug is in the amorphous state, it becomes thermodynamically unstable and during storage it tends to re-crystallize. This occurs when there are traces of crystalline drug left in the solid dispersion which recrystallizes the amorphous drug substance by acting as a nucleating agent [13]. To prevent this, the principal point is to ensure that RAD001 is completely transformed from its crystalline state to an amorphous state subsequently improving physical stability and dissolution performance of the ES NP. In another scenario, in solid dispersion a drug is presented as molecular or amorphous state for higher solubility and dissolution to be achieved. In a supersaturated condition however, there is a risk of drug crystallization. A decline in drug concentration can be retarded to different degrees based on the ability of the dissolved polymer to inhibit drug precipitation from the supersaturated state. When drug concentration declines gradually, it increases the inhibitory effectiveness of drug precipitation a cardinal requirement in maintaining drug supersaturation [14]. In this regard we leveraged SOL® an amphiphilic co-polymer being a strong solubilizer and matrix former to be the most effective in maintaining the stability of supersaturation by a reduction in crystal nucleation and growth. The qualitative characterisation known as a ‘spring and parachute’ approach has been identified for typical dissolution profiles of an amorphous solid dispersion as confirmed by our results whereby it is defined by a fast-initial build- up of API supersaturation followed by retardation of precipitation [14]. SOL® was also selected to enhance the solubility of poorly soluble RAD001 and to form NP in combination with PVA. SOL® is also known to have P-glycoprotein (p-gp) inhibition effects which may lead to increased drug delivery to the brain [15–17].

PVA was selected to enhance mechanical properties of PVA-SOL® by enhancing cross-linking of the NP to form stronger gels by tuning of crystallization, hydrogen bonding as well as the final hydrogel properties via exposure to repeated freeze–thaw (F/T) cycles. F/T of PVA was pioneered by Peppas demonstrating that upon repeated F/T cycles, PVA gels become more strengthened due to phase separation and crystallization [18]. The main parameters that influence the strength of the PVA-SOL® NP is the molecular characteristics;- molecular weight and degree of hydrolysis as well as gelation properties such as, duration, temperature of F/T cycles and number of F/T cycles [18]. Therefore, the objective of this study was also to explore the F/T on the combination of PVA-SOL® NP encapsulated with RAD001 and its effects in achieving a sustained release and improved solubility of RAD001 in the tumour microenvironment. The samples were exposed to repeated F/T cycles to determine the ability of SOL® and PVA to further efficiently encapsulate RAD001 in a PVA-SOL® based NP drug delivery system. RAD001 is then quantified via our developed HPLC method to ensure that quantification of RAD001 in biological matrices is made possible. A research of various different articles suggests different methods on the quantification of RAD001, for example, UV spectrophotometry, LC-MS, and HPLC [2,19]. The advantage of this developed method is that it is accurate, precise, sensitive, with a high recovery and short run time. To demonstrate these objectives, particle size analysis, encapsulation efficiency, drug release, differential scanning calorimetry (DSC) and HPLC tests were performed.

2. Materials and method

2.1. Materials

RAD001 (Everolimus) (>99 % purity) was purchased from LC

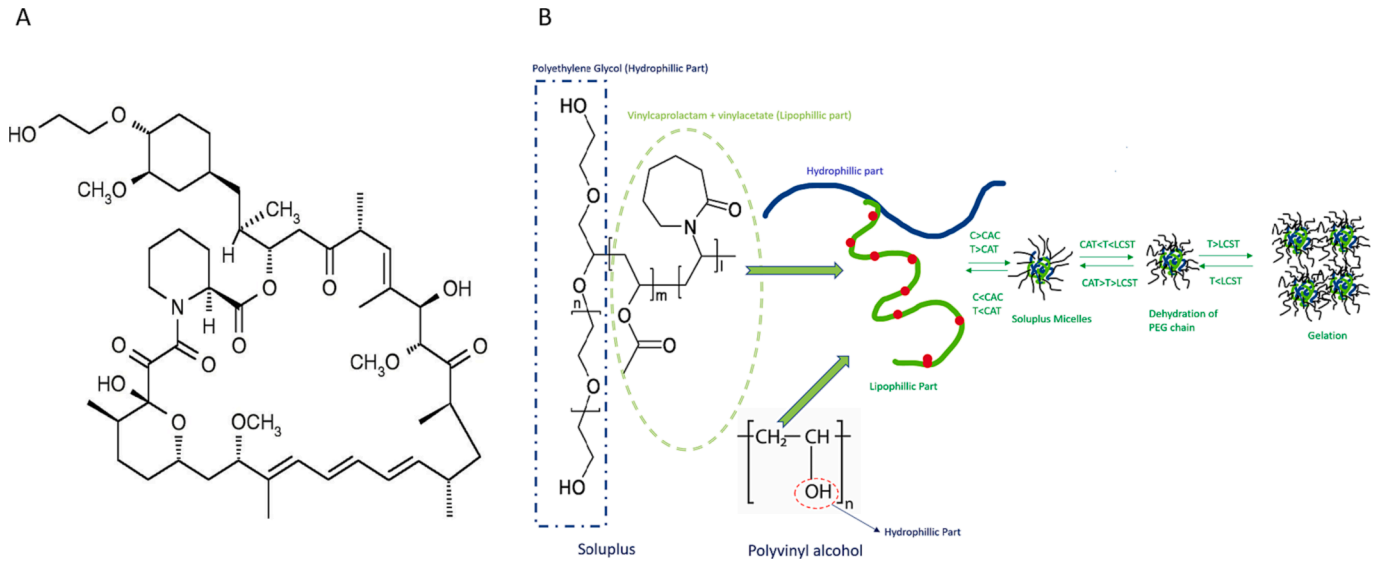

Fig. 1. A: chemical structure of rad001 1b). schematic representation of rad001 loaded pva-sol® NP; CAC- critical aggregation concentration; CAT-critical aggregation temperature; CMC- critical micelle concentration; CMT- critical micelle temperature [8] [28]

Laboratories (Woburn, MA, USA), Soluplus® was purchased from BTC Europe GmbH -A BASF Group Company, PVA (Mw = 13,000–23,000 g/mol, 87–89 %). The molecular weight of PVA was kept constant at 23,000 g mol^{-1}. Acetonitrile (CHROMASOLV™, gradient grade, for HPLC, ≥99.9 %) and methanol (CHROMASOLV™, gradient grade, for HPLC, ≥99.9 %) was purchased from Honeywell Research Chemicals, which were used for preparing mobile phase and diluent. De-ionised water was obtained from Milli Q water purification system and met the European Pharmacopeia requirements. The stock and standard solutions were prepared using diluent consisting of (80:20, v/v) methanol: de-ionised water. All other chemical reagents were analytical grade purchased from commercial suppliers.

2.2. Optimisation of PVA, SOL® and RAD001 concentration via electrospraying

Preliminary studies were performed to examine the formation of NP. To obtain the NP, a series of experiments with different SOL® concentrations (10 %, 15 % and 20 %), PVA concentrations (1 %–5 %) and RAD001 contents (0.6 %w/v) per weight in volume as listed in Table 1 was tested. The optimisation of SOL®, PVA and EVR concentration was then carried out based on the full factorial design generated by Minitab Statistics software Version 17 with three varying parameters comprising the SOL® concentration, PVA concentration, and RAD001 concentration. The criteria applied for the final selection of the PVA-SOL®-RAD001 concentration was based on the SEM images of the NP to obtain proper uniform spheres post the F/T cycles and *in-vitro* drug release results.

2.3. Polymer solution and polymer drug solution preparation

PVA and SOL® polymeric solutions were prepared using distilled water and ethanol. For PVA-SOL® polymeric solution 2.5 %w/v and 25 %w/v of each polymer was prepared using 4 mL of distilled water under a magnetic stirring rate at 500 ± 10 rpm. The solution was left to stir for 4 h with no heat applied until a homogenous clear solution was obtained for electro-spraying. When the PVA-SOL® solution was completely dissolved, 1 mL of ethanol was added to the final homogenous solution and stirred for 2 h to obtain a final concentration of 2 % and 20 % PVA-SOL® polymeric solution. Following optimisation of the PVA-SOL® polymeric solution the RAD001 stock solution was added.

The RAD001 stock solution was prepared by dissolving 30 mg of RAD001 into 1 mL of ethanol (ETOH). The stock solution was added into the final PVA-SOL® polymeric solution dropwise to obtain a final drug-polymer concentration of 0.6 %w/v under continuous stirring at 500 rpm ± 10 rpm. The PVA-SOL® NP containing RAD001 are referred to as PVA-SOL®-RAD001.

Table 1
The varying concentrations of Soluplus® (SOL®) and Polyvinyl alcohol (PVA) in conjunction with the established Everolimus (RAD001) concentration prepared for Electrospraying, with the molecular weight (MW) of PVA maintained at 23,000 g $mol^{-1.}$ to optimise the formulation.

Concentration of SOL® (%w/v)	Concentration of PVA (% w/v)	Weight of RAD001 in 5 mL solution
10	1	30 mg
	2	
	3	
	4	
	5	
15	1	30 mg
	2	
	3	
	4	
	5	
20	1	30 mg
	2	
	3	
	4	
	5	

2.4. Electrosprayed nanoparticle preparation

A horizontal electrospinning machine (Spraybase®, Ireland) was used to produce the electrosprayed NP. The PVA-SOL® solution was poured into a 15 mL conical centrifuge tube and placed inside a pressure vessel that was connected to a blunt stainless steel 25 G nozzle via a polytetrafluoroethylene (PTFE) tube. The tip of the nozzle was mounted at 15 cm vertically above a stainless-steel collector plate. The PVA-SOL® NP was prepared using a voltage of 16.5 ± 0.5 kV and a pressure of 0.050 bar to emit a positively charged single jet from the tip of the nozzle. Each PVA-SOL® polymeric solution concentration without RAD001 (Table 1) was electrospun for 8 h. The stainless-steel collector plate was wrapped in standard aluminium foil and the tip of the needle to the collector distance was set to 15 cm. Temperature and relative humidity recorded were in the ranges 25–30 °C and 61–65 %, respectively.

Following the optimisation of PVA-SOL® concentrations to produce NP by electro-spraying, encapsulation of RAD001 in the PVA-SOL® NP (Table 1) was performed using similar electrospraying parameters for the PVA-SOL® solutions. The F/T step was performed (Table 2). For the initial freezing step, the NP were immediately placed in a −80 °C freezer for 24 h and subsequently placed in a −20 °C refrigerator for 24 h. This step was repeated 6 times and was labelled as the 6 freezing (6F) cycle. After completing the 6F cycles, the frozen NP were thawed at room temperature (RT) for 30 min until the NP were de-frosted and re-frozen at −80 °C for 30 min. This step was repeated 3 times and was labelled as the 3 thawing (3 T) cycle. However, the NP showed no effect with the 6F/3T cycles, therefore the number of freezing steps was increased to 9F cycles and 3F cycle.

2.5. Methods for HPLC validation

2.5.1. Chromatographic conditions

Analytical separation was performed using the Waters - HPLC 2695 system equipped with an in-built autosampler, binary pump, photo diode array (PDA) Detector, an injection system (Rheodyne) with a 10 µl injection loop, thermostat and in-line degasser. Chromatographic software Empower 2 was used for data analysis, processing and interpretation. The column employed for analysis is a Licrospher stationary phase C18 RP (4 mm × 250 mm packed with 5 µm particle size) from Agilent Technologies at an adjusted temperature of 50 °C ± 2 °C. The chromatographic elution employed was isocratic at a flow rate of 1 mL/min with an established mobile phase of (90:10, v/v) acetonitrile: de-ionised water and the PDA detection was performed at 278 nm. The mobile phase was sonicated to remove air bubbles prior to placing on to HPLC reservoir. The autosampler was set at 5 °C.

2.5.2. Mobile phase and diluent optimization

Mobile phase was optimized according to the Design of Experiments (DOE) generated by Minitab Software. Based on the DOE, initially,

Table 2
Electrosprayed nanoparticles (NP) PVA-SOL®-RAD001 exposed to varying freeze–thaw (F/T) cycles used in this study to study the effects of F/T nanoparticles to achieve uniform sized NP and a sustained release for *in vitro* studies.

	Method 1 (6F/3T)	Method 2 (9F/3T)
Number of freezing cycle (F)	6	9
Temperature 1 (°C)	−80	−80
Temperature 2 (°C)	−20	−20
Number of thawing cycle (T)	3	3
Thawing temperature (°C)	RT	RT
Re-freeze temperature (°C)	−80	−80

mobile phase containing ammonium acetate, as buffer was attempted, (50:50, v/v) ammonium acetate: acetonitrile with the pH adjusted to 6.5 using orthophosphoric acid. However, with the use of buffer, a rising baseline was observed for every second injection, high peak tailing and peak fronting as well as inconsistent number of theoretical plates. Separations were then carried out using acetonitrile: water, methanol: acetonitrile, methanol: water with different organic ratios. The final mobile phase established was with a ratio of (90:10, v/v) acetonitrile: water where all acceptance criteria was met for the system suitability performed. This established mobile phase produced well separated peaks from RAD001 (Fig. 2). Prior to performing analysis, the mobile phase was sonicated for 5 min to remove air bubbles, and was filtered through 0.45 μm Whatmann filter. The mobile phase was passed through the column at an established flow of 1 mL/min at a set temperature of 50 °C ± 2 °C. The retention time of RAD001 was observed at 2.916 min with a *cis*-isomer observed at 3.15 min as per manufacturers Certificate of Analysis (COA) and stable baseline was observed. The established injection volume was set at 10 μl with a total run time set at 6 min. Based on the chromatogram, the mobile phase of (90:10, v/v) acetonitrile: de-ionised water was established. 900 mL of acetonitrile and 100 mL of de-ionised water was used to make up the mobile phase. For diluent preparation, 800 mL of methanol and 200 mL of de-ionised water (80:20, v/v) was mixed and sonicated.

2.5.3. Preparation of stock solution and working standard solution

RAD001 stock solution with a concentration of 1000 μg/mL was prepared by accurately weighing 10 mg of RAD001 powder onto a weigh boat. The powder was the transferred into a 10 mL amber volumetric flask. Subsequently, 5 mL of diluent was added to the volumetric flask, swirled and allowed to sit for 10 min to ensure the RAD001 was completely dissolved. The solution was then made up to the mark with diluent and inverted 10 times to obtain a homogenous stock solution. From the prepared stock solution, a serial dilution was performed to obtain 6 working concentration range of 5, 50, 75, 100, 125 and 150 μg/mL of RAD001.

2.5.4. Method validation procedure for HPLC

The method was developed according to the International Conference of Harmonization (ICH) guidelines and was validated for linearity, precision, accuracy, specificity, limit of detection (LOD), limit of quantification (LOQ) and robustness in accordance with standard procedure. [2,20]. Optimisation of chromatographic separation with the aim of obtaining a well separated RAD001 peak with respect to the chromatographic parameters such as flow rate, sample volume, detection wavelength, temperature and mobile phase composition.

2.5.5. Linearity and repeatability

Under the established experimental conditions, the standard calibration curve was prepared with six calibrators within a concentration range of 25–150 μg/mL for RAD001. A calibration curve of peak area versus RAD001 drug concentration was studied and were treated by linear square regression analysis. 10 μl of each calibrator was injected under the established chromatographic conditions and each chromatogram was recorded. The correlation coefficient value observed was ($r^2 =$ 0.999). Six injections of the prepared 100 μg/mL were injected and the peak area was measured. The relative standard deviation (%RSD) was less than 2 % confirming that the method developed is repeatable. Table 3 shows the summarised validation parameters.

2.5.6. Precision and specificity

The precision was studied with respect to interday and intraday replication analysis. In relation to interday precision, the analysis was repeated for three consecutive days at a concentration similar to intraday precision with repeatability calculated from six replicate injections. The intraday precision analysis was carried out on the same day at different time intervals. Precision was expressed by %RSD of the peak of interest, in this case RAD001. Specificity of the method was measured based on the presence of interference/excipients at the main peak of interest and this was observed by the samples that were injected as blanks, samples and standard solutions.

Table 3
Validation Parameters according to ICH guidelines for HPLC method development for Everolimus (RAD001) summarised [20].

Validated Parameters	RAD001
Concentration Range Linearity (μg/mL)	25–150
Correlation coefficient	0.999
Linear Regression Equation	y = 2E + 07x
LOD	4.419
LOQ	12.575
Intraday Precision %RSD (n = 6)	0.40 %
Interday Precision %RSD (n = 6)	0.16 %
Number of Theoretical Plates	>9000
Tailing Factor	1.17
Retention Time	2.916 min

*Note: LOD:Limit of detection, LOQ: Limit of Quantification, RSD: Relative Standard Deviation.

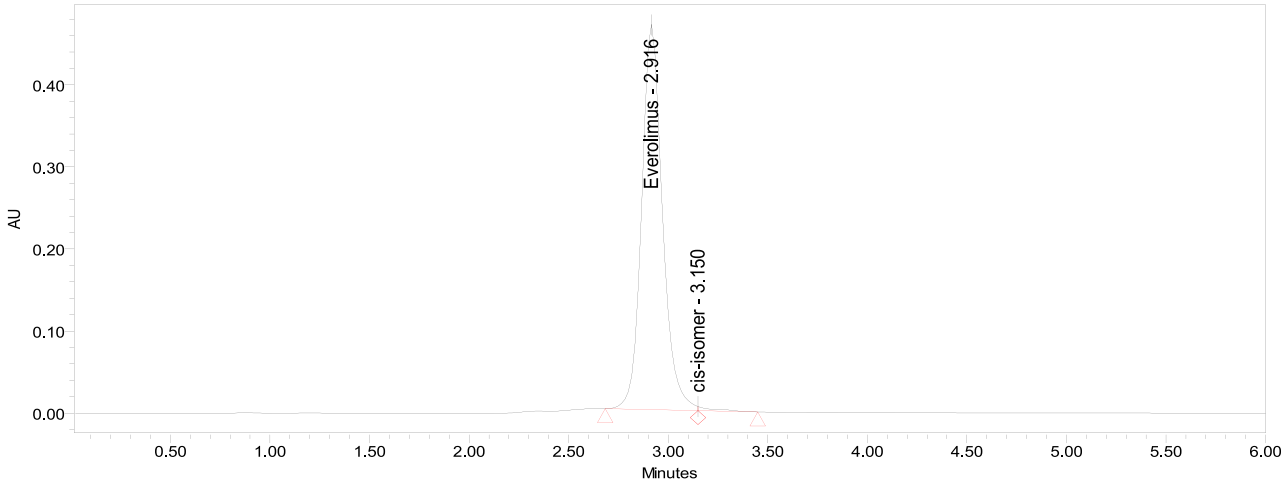

Fig. 2. Representative chromatogram of Everolimus (RAD001) diluted in 800 mL of methanol and 200 mL of deionised water (80:20, v/v) diluent with a final concentration of 1000 μg/mL. The *cis*-isomer at retention time 3.15 min confirms that the active ingredient (RAD001) is comparable to the manufacturer's chromatogram.

2.5.7. Accuracy

To determine the accuracy of RAD001, the standard addition method was employed to calculate the % recovery of RAD001. Based on the sample analysed at 100 μg/mL, a known amount of drug standard was added at a % level of 50, 300 and 350 (50, 300 and 350 μg/mL). The % recovery of RAD001 was analysed according to ICH guidelines. The analysis was done in-triplicate and the accuracy was determined by the % recovery calculated. The % accuracy data is tabulated below (Table 4).

2.5.8. Limits of detection, quantification and robustness

Limits of Detection and Quantification was determined and calculations was made with the following equations below: -

$$LOD = 3.3\,\sigma/S \quad (1)$$

$$LOQ = 10\,\sigma/S \quad (2)$$

Where σ is the standard deviation of the response (an estimate from the standard deviation of the y-intercept of the regression line) and S is the slope of the standard curve [2,20,21]. The robustness of the method was measured based on the ability of the method to remain unchanged by small and deliberate variations in method parameters such as change in column, mobile phase, sample instrument and gradient.

2.5.9. Forced degradation studies of RAD001

Forced degradation studies was performed by subjecting 10 mg of RAD001 to acidic, alkaline, neutral, oxidising, thermal and photolytic conditions.

Acidic Degradation

From the prepared stock solution, 1 mL of the stock was taken and added to 2 N HCL and the mixture heated under reflux conditions at 60 °C for 30 min. The solution was neutralised with the addition of 1 mL of 2 N NaOH. The sample was left to cool to room temperature and diluted with diluent to obtain a final concentration of 100 μg/mL.

Alkaline Degradation

From the prepared stock solution, 1 mL of the stock was taken to 1 mL of 2 N NaOH and the mixture was heated under reflux at 60 °C for 30 min. The solution was neutralised with the addition of 1 mL of 2 N HCL. The sample was left to cool to room temperature and diluted with diluent to obtain a final concentration of 100 μg/mL.

Neutral Degradation

From the prepared stock solution, 1 mL of the stock was taken and heated under reflux at 60 °C overnight. The sample was left to cool to room temperature and diluted with diluent to obtain a final concentration of 100 μg/mL.

Oxidising Degradation

Oxidising degradation was performed using hydrogen peroxide as the cancer microenvironment contains high levels of hydrogen peroxide. 1 mL of stock solution was added to 1 mL of 20 % hydrogen peroxide solution and heated to 60 °C for 30 min. The sample was left to cool to room temperature and diluted with diluent to obtain a final concentration of 100 μg/mL.

Thermal Degradation

Thermal degradation studies were performed by accurately weighing 10 mg of RAD001 pure in a glass vial and exposing the weighed drug to two different temperatures 100 °C and 60 °C respectively for 6 h. The sample was left to cool to room temperature and diluted with diluent to obtain a final concentration of 100 μg/mL.

UV degradation

UV degradation was performed by weighing10 mg of RAD001 in a glass vial and exposing to sunlight for 7 days. The sample was left to cool to room temperature and diluted with diluent to obtain a final concentration of 100 μg/mL.

The aim of the forced degradation study above was to determine the presence or formation of new impurities when the compound/API was exposed to different stress conditions. The samples were run under the above-mentioned conditions and the data was processed and collected using the Empower 2 software. A PDA detector was used to determine the drug purity.

3. Physico-chemical characterisation

3.1. Encapsulation efficiency and morphology of PVA-SOL®-RAD001 NP

The PVA-SOL®-RAD-001 NP were dissolved in deionised water. The dissolved nanoparticles were then diluted in methanol to dissolve free RAD-001. Free RAD-001 was then separated from the PVA-SOL®-RAD-001 NP by using a microfilter with a pore size of 0.45 μm. The free RAD-001 was then assayed by HPLC as described above. The encapsulation efficiency was determined using equation (3).

$$EE = \frac{W_{\mathrm{RAD-001-loaded-Nanoparticles}}}{W_{\mathrm{total-RAD001}}} \quad (3)$$

The particle size of the PVA-SOL®-RAD001 NP were determined by the zeta sizer (Malvern Panlytical, Malvern, UK) using dynamic lights scattering at a wavelength at 633 nm (nanometers) and the scattering angle was fixed at 90°. The morphology of the PVA-SOL®-RAD001 NP was examined using a TESCAN SEM (Brno, Czech Republic). The sample was mounted on a silver stub under vacuum conditions and sputter-coated with gold in a Baltec SCD 005 sputter coater for 110 s at 0.1 mbar vacuum to yield a uniform coating of ca. 110 nm on the stub. The surface morphology was then viewed using the SEM instrument.

3.2. Differential scanning calorimetery

For thermal analysis a Pyris Perkin Elmer (TA instruments, Inc) was used. For each sample, a heating rate of 10 °C/min was applied to each sample under the purging of nitrogen gas. Three cycles (heat-cool-heat) were tested for each sample. The samples were initially heated from 20 °C to 250 °C and this was labelled as cycle 1. Cycle 2 involved cooling

Table 4
% Recovery of spiked Everolimus (RAD001) by the standard addition method to determine accuracy. Each level was repeated three times and the accuracy was demonstrated by % recovery. The accuracy of the developed analytical process determines the degree of closeness between the derived values and the genuine values also defined as % recovery.

Level	Sample Concentration (μg/mL)	Amount of Standard Added (μg/mL)	Total Concentration (μg/mL)	Found Concentration (μg/mL)	%RSD	% Recovery
50	100	50	150	123.94 124.48 124.83	0.4	83 %
300	100	200	300	326.16 328.72 328.59	0.4	101 %
350	100	250	350	340.64 342.32 340.93	0.4	100 %

*%RSD = Relative Standard Deviation.

of the sample in the furnace back to 20◦C. In cycle 3 the sample was heated again from 20 °C to 250 °C. The degree of crystallinity (Xc) of the hydrogel samples from the endothermic area was calculated based on the following equation [22]:

$$Xc = \Delta Hf/\Delta Hf_o \quad (4)$$

where ΔHf represents the measured enthalpy of fusion of the PVA microsphere and ΔHf_o is the thermodynamic enthalpy of fusion for 100 % crystalline PVA ($\Delta Hf_o = 138.60$ J/g).

3.3. In vitro dissolution studies

The tumour microenvironment is also known as the extracellular environment adjacent to tumours [23]. This microenvironment has an acidic pH and a high concentration of hydrogen peroxide (H_2O_2) [24]. The *in vitro* RAD001 release kinetics from the NP containing PVA-SOL® at 10 % 15 %, and 20 % (w/v) SOL® and a constant of 2 % (w/v) PVA respectively was evaluated using the USP (United States Pharmacopeia) Apparatus 1 method. PVA was kept constant at 2 %, because any concentration higher than 2 % (w/v) of PVA formed beaded fibres. The final concentration of RAD001 in the NP was 600 mg/mL. The *in vitro* buffers were prepared to recapitulate the pH of the tumour microenvironment (pH 6.8) and the tumour itself (pH 7.2–7.4). However, the intracellular pH of tumour cells also known as the 'leading edge zone' is maintained within a pH range of 7.2–7.4 [23]. Therefore, to study the stability and degradation of the PVA-SOL®-RAD001 NP were carried out in different pH values (pH 7.4 and 6.8) according the USP methods of preparation. The dissolution studies were performed in -triplicate for each buffer pH respectively. Approximately 0.2–0.4 g of the dried NP was placed into a rotating basket containing 250 mL of releasing medium (PBS) phosphate buffer and stirred at 50 rpm for a total of 5 days at 37 ± 1 °C and for each buffer (pH 7.4 and 6.8). A total of 2 mL of aliquot was withdrawn at different time intervals of 10, 20, 30, 40, 50, and 60 min, followed by each hour for the first 8 h and then subsequently every 24 h for a total of 5 days until no further changes in release of RAD001 was observed on the HPLC chromatogram. Each collected aliquot was replaced with fresh 2 mL of PBS. Each formulation was tested in triplicate to ensure repeatability. The concentration of RAD001 in the samples collected was assayed in real-time by HPLC (Waters Alliance 2695) system. The mobile phase was composed of water:acetonitrile (10:90, v/v) at a flow rate of 1 mL/min and absorption wavelength of 280 nm.

3.3.1. RAD001 release kinetics

The release kinetics of RAD001 encapsulated in PVA-SOL-RAD001 NP in phosphate buffer (PBS) pH 7.4 and 6.8 was determined via data collected from the dissolution release profile. The data was the input into the DDSolver software and tailored into zero-order, first-order, Higuchi, Korsmeyer–Peppas, and Hixson–Crowell models (Five Kinetic models) to demonstrate the drug release kinetics. The different kinetic models signify different drug release kinetics from the optimized formulation.

4. Results and discussion

4.1. HPLC validation

The HPLC conditions were optimised according to the ICH guidelines to obtain proper peak parameters such as tailing factor, number of theoretical plates, signal/noise ratio, proper peak shape and resolution. To ensure optimum HPLC conditions to detect the presence of RAD001, several preliminary experiments were carried out for example;- using a combination of different mobile phases which includes buffers such as ammonium acetate, formate and sulphate buffers, TFA, formic acid and acetic acid, and organics such as methanol and acetonitrile both with and without (1 % TFA), different elution approaches such as isocratic and gradient, varying column temperatures from ambient to 50 °C, different flow rates 0.2–1 mL/min. After preliminary tests, the isocratic flow was established with the following conditions: - acetonitrile:water 90:10 with the Licrospher C18 RP (4 mm × 250 mm packed with 5 μm particle size) from Agilent Technologies at a flow rate of 1 mL/min. The column oven temperature was set at 50 °C and sample temperature was maintained at 5 °C. RAD001 was measured using a PDA detector at 280 nm. The observed retention time was 2.916 ± 0.01 min. However, it is also worthy to note that retention time shifts can also occur with change in mobile phase, instrument conditions and column care. The total sample analysis time was 6 min for the established mobile phase and column used. Different mobile phases yield different retention times and run times at a maximum of 30 min depending on the organic content and buffer used. The run time was shortened to 6 min, with the optimised mobile phase making this a cost-effective method. The tailing factor and number of theoretical plates was recorded as 1.22 and 11,003 confirming the efficiency of column performance. The parameters meet the requirements as outlined in the guidelines of the International Conference on Harmonization (ICH) Q8, Q9, Q10 and Q11.

Calibration curve

The calibration curve (supplementary material 1) showed good linearity in the concentration range tested from 25 to 150 μg/mL for RAD001, and the results yielded a linear method with a correlation coefficient of 0.999. Linear regression was used to compare the sample concentration (X) with the peak area of the RAD001 HPLC (y).

Precision and Accuracy

The results for both intraday and interday precision was evaluated based on the %RSD. Intraday precision was analysed at different time points on the same day. The %RSD for intraday was calculated to be 0.4 %. For interday precision, the analysis was carried out over a period of three days at the same concentration as the intraday precision. The % RSD calculated for interday was 0.8 %. The method accuracy was calculated to be between 83 %−101 % with a mean % recovery of 95 % for RAD001 confirming the accuracy of the method.

LOD and LOQ

The limit of detection and limit of quantification for RAD001 was found to be 4.149 and 12.575 μg/mL, which indicate the sensitivity of the method. Selectivity of the method was demonstrated by the absence of any interfering peaks at the retention time of the drug. Validated method was applied for the determination of RAD001 in commercial formulations. The method is observed to be selective based on the absence of interfering peaks in the chromatogram. The % assay for RAD001 was found to be 99.82 % indicating good compliance with the label claim.

4.2. Forced degradation study

The degradation of RAD001 was studied under different stress conditions. RAD001 showed stability under thermal conditions and UV degradation. However, post alkaline treatment, RAD001 showed complete degradation as per Fig. 3(b), and 87 % of RAD001 degraded under acidic conditions (2 N HCl, 60 °C, 30 min). Post oxidizing treatment (20 % H_2O_2, 60 °C, 30 min), 96 % of the drug showed degradation. As part of mimicking the tumour microenvironment containing H_2O_2, the encapsulated RAD001 in the optimised formulation with 9F/3T cycles and no F/T cycles were stressed under the same oxidizing treatment. 5 % of the drug degraded showing a marked decrease confirming that PVA-SOL® protects the encapsulated RA001 from oxidative stress with the formation of a new peak. (Supplementary Material). The % of drug degraded after thermal conditions were less than 1 %. Based on the method developed, the RP-HPLC with PDA detection method is linear, precise, accurate and robust to quantify RAD001 in electro-sprayed PVA-SOL® was developed and validated. Based on the degradation profile of RAD001 under various different stress conditions, no interference was observed when quantifying RAD001. Therefore the method can be defined as a stability indicating method owing to its ability to quantify

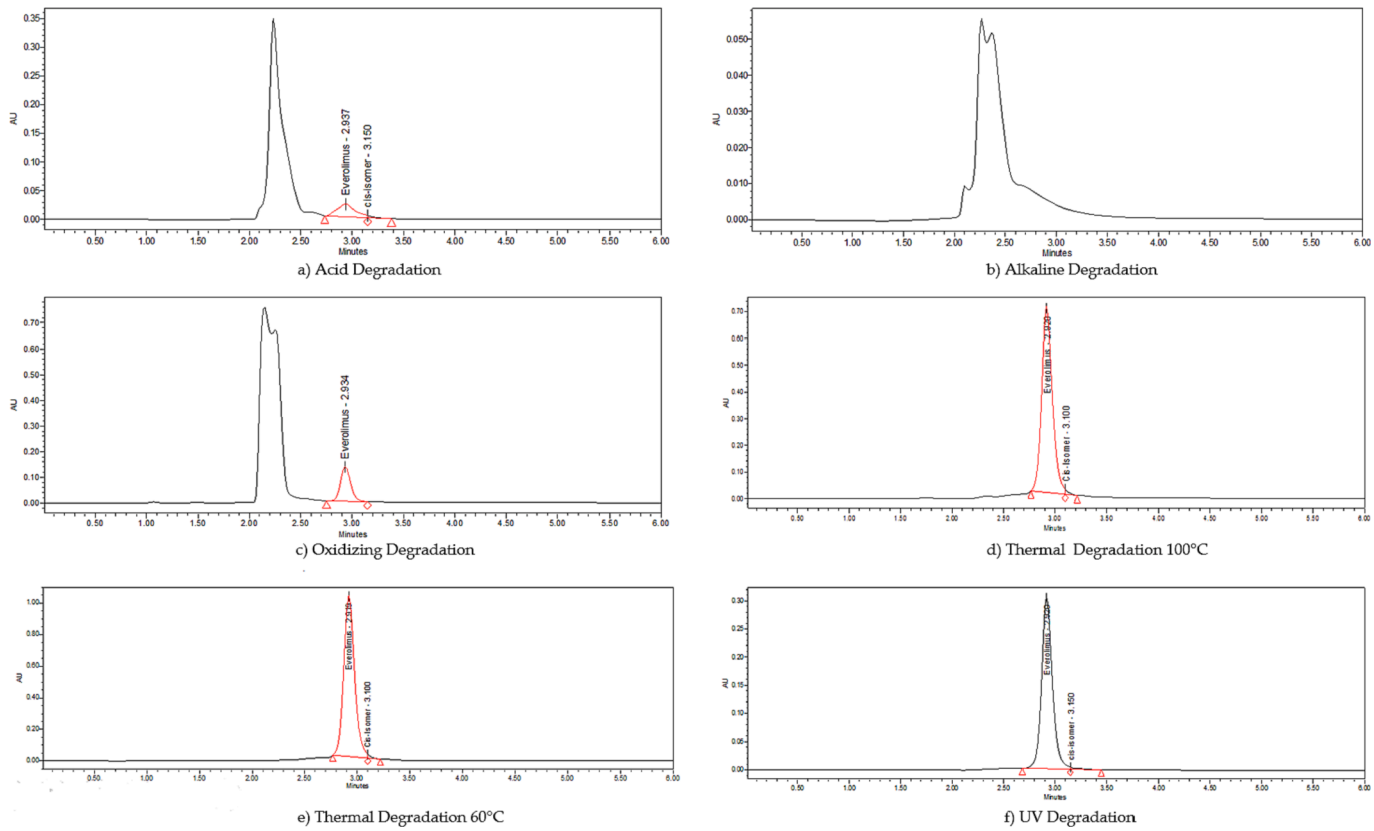

Fig. 3. Chromatograms of RAD001 subjected to different stress conditions. A) Acidic Degradation; B) Alkaline Degradation; C) Oxidising Degradation; D) Thermal Degradation 100 °C; E) Thermal Degradation 60 °C; F) UV Degradation.

RAD001 accurately and precisely free from degradation products, polymers and process impurities (Fig. 3) [25].

4.3. *Optimisation of PVA-SOL®-RAD001 concentration*

The optimisation of electro-sprayed NP of PVA-SOL®-RAD001 was systematically assessed based on concentration and molecular weight. Based on the results observed, the following material grades and concentrations yielded the optimum strength and viscosity to achieve the desired geometry for the NP: PVA Mowiol grade 18–88 with a concentration per weight in volume and molecular weight of 2 % and 23, 000 g/mol respectively, 20 % SOL® the triblock graft copolymer ((polyvinyl caprolactam–polyvinyl acetate–polyethylene glycol (57:30:13)) with - molecular weight of 90,000–140,000 g/mol and 0.6 % per weight in volume of RAD001 achieved the optimum strength and viscosity to achieve the desired geometry for the NP.

SOL® concentrations lower than 10 % was not viscous enough to electrospray resulting in the whipping mode and still liquid droplets when electro-sprayed on the collector plate, unable to form NP [26]. The decrease in chain entanglements for lower viscosity solutions within a drop of the solution is insufficient for stabilisation of the structure of the particle formed causing a loss of shape when it impacts the collector plate. In comparison, concentrations of SOL® above 20 % was too viscous forming beaded nanofibres. This is due to the increased number of chain entanglements which consequently stabilises the jet formation. This prevents jet break up caused by increased surface tension, therefore producing beaded fibres [9]. Based on the sol–gel transition ($T_{SOL-gel}$) properties, the $T_{SOL-gel}$ of SOL® below 10 % was above body temperature of 37 °C whereas concentrations above 20 % was too viscous making it unsuitable as a drug delivery system. The concentration of PVA was maintained at 2 % to prevent agglomeration of the NP. Concentrations of PVA above 2 % formed beaded nanofibres. Therefore, the achieved polymer concentration range of 20 % SOL® and 2 % PVA was established for the NP formation.

4.4. *Appearance of PVA-SOL® hydrogels*

The established concentration in this study of PVA and SOL® is 2 % and 20 % respectively. SOL® is a thermosensitive non-linear co-polymer composed of polyvinyl caprolactam–polyvinyl acetate–polyethylene glycol (57:30:13) ((PEG-*g*-(PVAc-co-PVCL)) with a molecular weight of 140, 000gmol^{-1}. SOL® is slightly transparent at either dilute or high concentrations, but at intermediate concentrations it is highly opalescent suggesting that the optical appearance of SOL® is concentration depended. [27].

The appearance characteristics at the sol and gel state of the PVA-SOL® mixture in phosphate buffer (200 mM, pH 7.4 and pH 6.8) as per Fig. 4A was examined. Based on our study, at 25 °C the PVA-SOL® sols were a colloidal light blue as reported by Wu, et al. [28] and opaque when heated at 37 °C due to the self-cross-linking properties of SOL®. This self-cross-linking was also observed during *in vitro* testing for the PVA-SOL®-RAD001 NP carried out at 37 °C as per Fig. 4B. The observed results suggest that SOL® forms uniform micellar structures and has a critical micelle concentration (CMC) of 7.6 mg/L below the gelling temperature [29].

4.5. *Encapsulation efficiency and morphology of PVA-SOL®-RAD001 NP*

The encapsulation efficiency of RAD001 was calculated based on the precipitation of free drug in the polymer solvent combination because RAD001 is practically insoluble in water. The calculated encapsulation efficiency was 99.71 % for the PVA-SOL®-RAD001 NP with 9F/3T cycles performed and 99.10 % for the PVA-SOL®-RAD001 NP with no F/T performed, which proves that RAD001 was efficiently encapsulated into

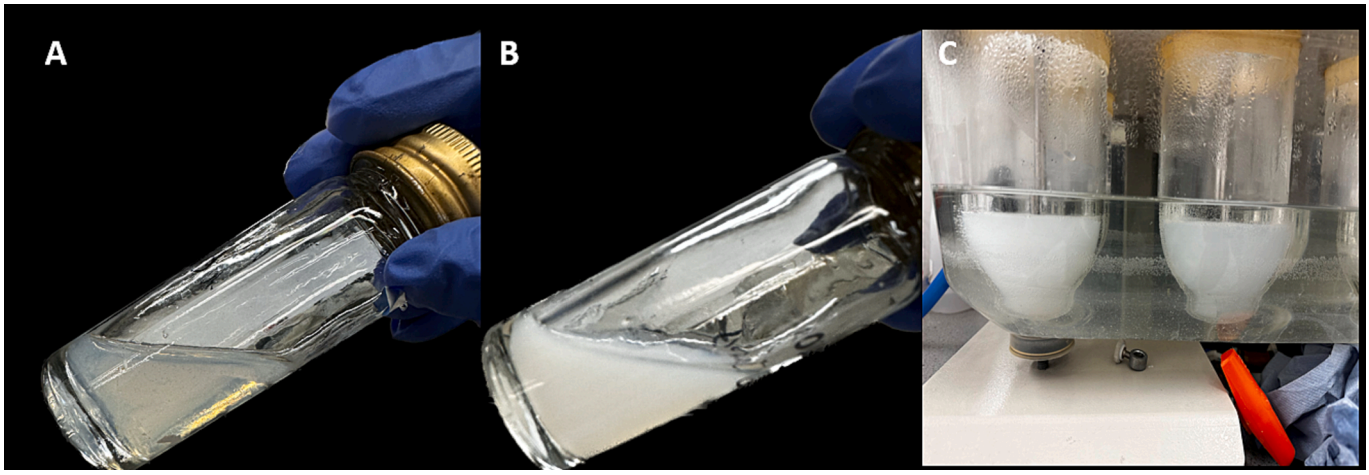

Fig. 4. Appearance and characteristics of PVA-SOL®-RAD001 NP. A) Appearance of 20 % SOL® in the sol state at 25 °C; B) Appearance of 20 % SOL® in the gel state at 37 °C; C) *in vitro* analysis of PVA-SOL®-RAD001 NP at 37 °C.

the PVA-SOL® NP. The particle size of the PVA, SOL® and PVA-SOL®-RAD001 NP with 9F/3T cycles and without F/T cycles were determined (in-triplicate) as well as the morphology using the Malvern Panlytical and the TESCAN SEM respectively. The mean hydrodynamic volume particle size (Fig. 5B) of drug-free PVA NP is 153 nm whereas for drug-free SOL® with 9F/3T and without F/T, the mean hydrodynamic volume particle size was recorded at 56 nm and 58 nm respectively. This could be due a phenomenon known as coalescence. These results are in line with a study conducted by Van Dyke et al. [30] who found that droplet coalescence at lower and prolonged freezing temperatures caused a decrease in particle size. As SOL® is able to self-assemble and is amphiphilic, the NP are in close contact in the superlattice. Therefore, coalescence can be facilitated, due to SOL® dense packing and proximity of the aligned facets that enable the crystal lattices to merge at low temperatures or below the bulk melting point [31]. Thus, during freezing, the variance in particle size is due to different coalescence behaviour rather than nucleation [30]. For the ES PVA-SOL®-RAD001 NP exposed to 9F/3T cycles, the mean hydrodynamic volume particle size slightly increased to 71 nm (Fig. 5B). In comparison to our previous paper, where the particle size was in the micrometer range, the electrosprayed nanoparticles of PVA-SOL®-RAD001 produced the nanometer range confirming the efficiency of the technique to provide a precise control over size and morphology. The morphology of the electro-sprayed PVA-SOL®-RAD001 was examined under SEM showing a uniform distribution of the spherical NP as per Fig. 5A.

4.6. DSC

Determination of the glass transition temperature (T_g) and the melting temperature (T_m) of the PVA-SOL®-RAD001 NP before and after freeze thawing was identified from the resultant thermographs. A DSC (Fig. 6) was carried out on pure PVA, pure SOL® and the electro-sprayed NP PVA-SOL®-RAD001 before and after the established freezing and thawing cycles. As observed on the DSC thermogram, peaks that are present below 100 °C reflects the content of water in each sample, a phenomenon caused by loss of adsorbed water [32]. Therefore, as seen on the DSC thermogram, the presence of shoulder like endothermic or exothermic peak within the range of 57 °C−64 °C denotes the loss of adsorbed water. The DSC analysis however was not sensitive enough to detect the presence of RAD001. This is then further analysed using the developed and validated HPLC method. As observed on the thermogram, the T_g value of SOL® and RAD001 increased from 89 °C to 117 °C in the ES PVA-SOL®-RAD001 NP with no F/T cycles performed. However, post 9F/3Tcycles, the T_g increased to 128 °C indicating an increase in hydrogen bonding post 9F/3T cycles, due to a decrease in free volume between the polymer chains causing an increase in the T_g value [33]. The PVA and SOL® molecular motion is slowed down when cross-linking happens during freezing and thawing cycles, and should not interact in the crystalline domain indicating an interaction between PVA-SOL®-RAD001. An increase in crystallinity would mean the formation of H-bonding and better orientation. The freezing and thawing cycles did not change the drugs melting event (T_m) of the NP PVA-SOL®-

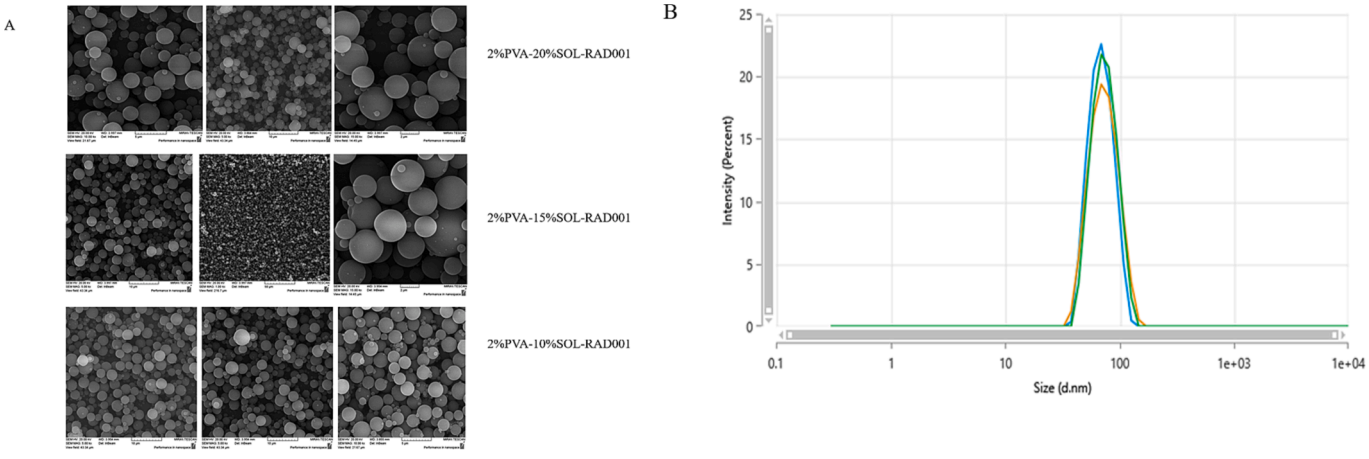

Fig. 5. A) SEM of the different concentrations of PVA-SOL®-RAD001 NP; B) Particle size of PVA-SOL®-RAD001 NP formulations.

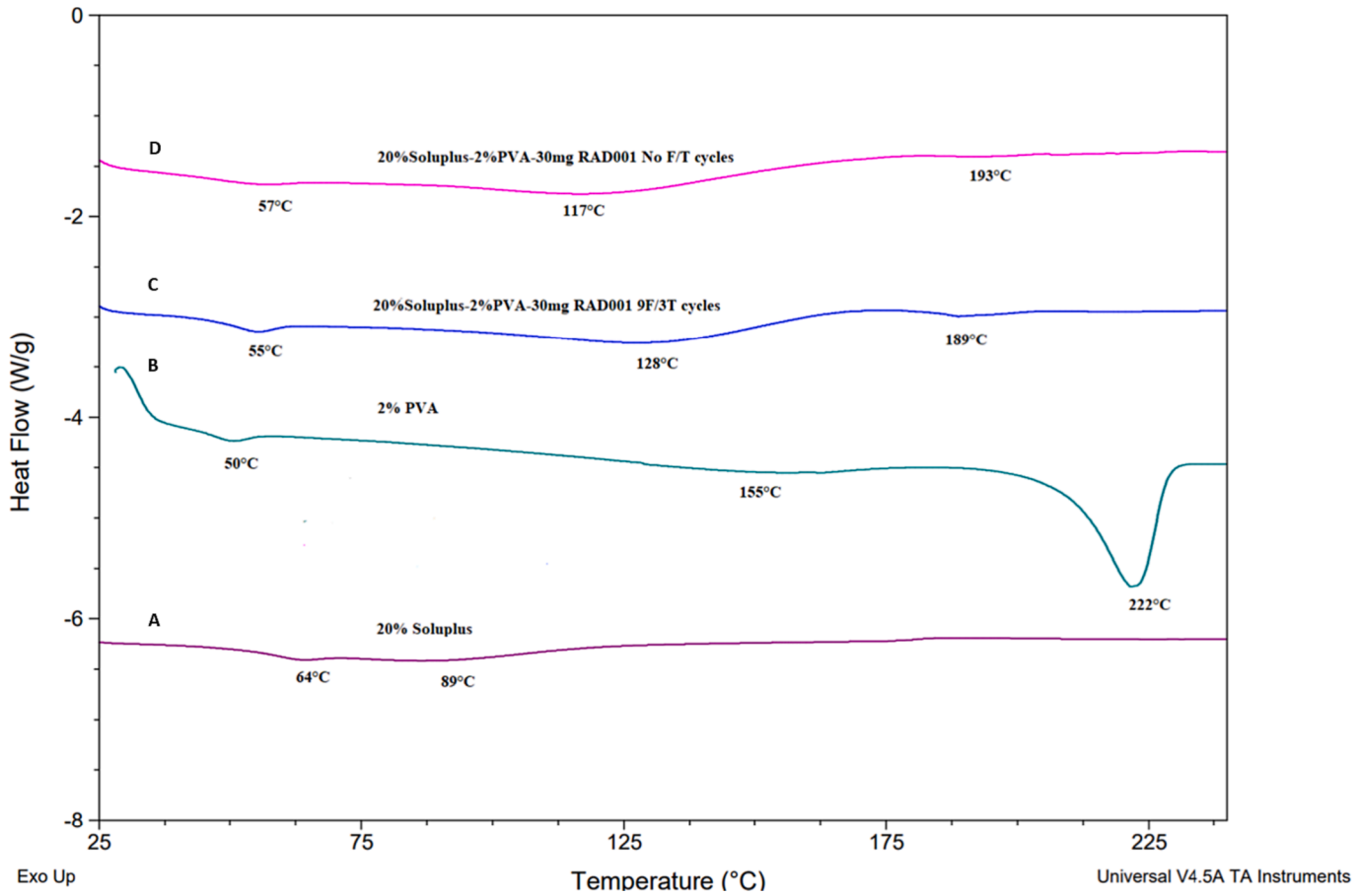

Fig. 6. DSC thermograms for A) 20 % Soluplus; B) 2 % PVA; C)physical mixture of 20 %SOL-2 %PVA-30 mg RAD001 9F/3T cycles; D) physical mixture of 20 %SOL-2 %PVA-30 mg RAD001 no F/T cycles.

RAD001 which remained in the same temperature range of 190 °C.

4.7. *In vitro* dissolution studies

The tumour microenvironment is also known as the extracellular environment adjacent to tumours [23]. In cancer this microenvironment is well known to have an acidic pH and a high concentration of hydrogen peroxide and is hypothesised to promote the migration and invasion of cancer [24,34]. *In vitro* studies have shown that the proliferation of a tumour is maximised at pH 6.8 which contributes to the acidity of the tumour microenvironment and the tumour cells itself remains neutral at a pH of 7.2–7.4 [35]. Release of RAD001 from the optimised formulation of 2 % PVA-20 % SOL® NP were assessed in different pH values (pH 7.4 and 6.8). The time taken to achieve a 50 % release of RAD001 in pH 7.4 buffer from the optimised NP exposed to 9F/3T and no F/T cycles were 20 min and 10 min respectively (Fig. 7). Drug release was observed for 8 h from NP exposed to 9F/3T cycles with a release of 92.8 % (N = 3) and 90.06 % release achieved within 40 min for the NP samples with no F/T cycles. The sustained release achieved for the 9F/3T sample produced by ES is attributed to the amphiphilic properties of SOL® that can form modified micellar structures for the encapsulation of RAD001 preventing a burst release. This is also known as the 'spring' phenomenon where the drug concentration increases with time [16]. There was no significant difference observed between the 15 %- and 20 % -SOL® concentration. However, for the 10 % SOL® concentration, the NP achieved 85.5 % (n = 3) release within 8 h post 9F/3T cycles, and 85.6 % (n = 3) release in 30 min for the NP that did not undergo F/T cycles. This could be due to lesser hydrogen bond cross-links when compared to the F/T samples resulting in the outer surface of the electrosprayed NP becoming loose from sampling consequently causing a much faster release.

In comparison, dissolution studies performed in pH 6.8 buffer for the optimised NP exposed to 9F/3T cycles, a 50 % release was achieved within 20 min and the for NP with no F/T cycles performed achieved 50 % release within 5 min. Fig. 7C indicates that an average of 86.1 % of RAD001 was released within 7 h for NP samples exposed to 9F/3T cycles, whereas an average of 84.9 % (Fig. 7D) was released within 50 min for the NP samples with no F/T cycles. The difference in release time for the F/T and non–F/T NP confirms the formation of hydrogen bonds cross-links between PVA and SOL® for the F/T NP. However, for the 10 % SOL® concentration, the NP achieved 89.4 % (n = 3) release within 3 h post 9F/3T cycles, and 85.8 % (n = 3) release in 30 min for the NP that did not undergo F/T cycles. For the 10 % SOL® concentration the immediate release observed for the 9F/3T samples non F/T samples in pH 6.8 in comparison to pH 7.4 could be attributed to the lower pH buffer triggering the degradation of the ester linkages between the hydrophobic and hydrophilic blocks of the polymeric micelles that form in the buffer to disassemble and release the drug molecule [36]. For optimised NP in both pH 6.8 and 7.4 buffer groups the release amount of RAD001 was improved is due to the diffusion blocking effect of stronger gel-strength confirming the stability of the ES NP to withstand the tumour microenvironment.

Table 5a and b indicates the model of best fit for RAD001 release profile for the different pH values. The calculation of the release profile was done using various kinetic models including zero-order, first-order, Higuchi, Korsmeyer-Peppas and Hixson-Crowell via the DDSolver software. For the optimised concentration of the NP that were exposed to 9F/3T cycles and no F/T cycles in pH 7.4 buffer, the First-Order model was the model of best fit ($R^2 = 0.8531$ and $R^2 = 0.9660$ respectively) for

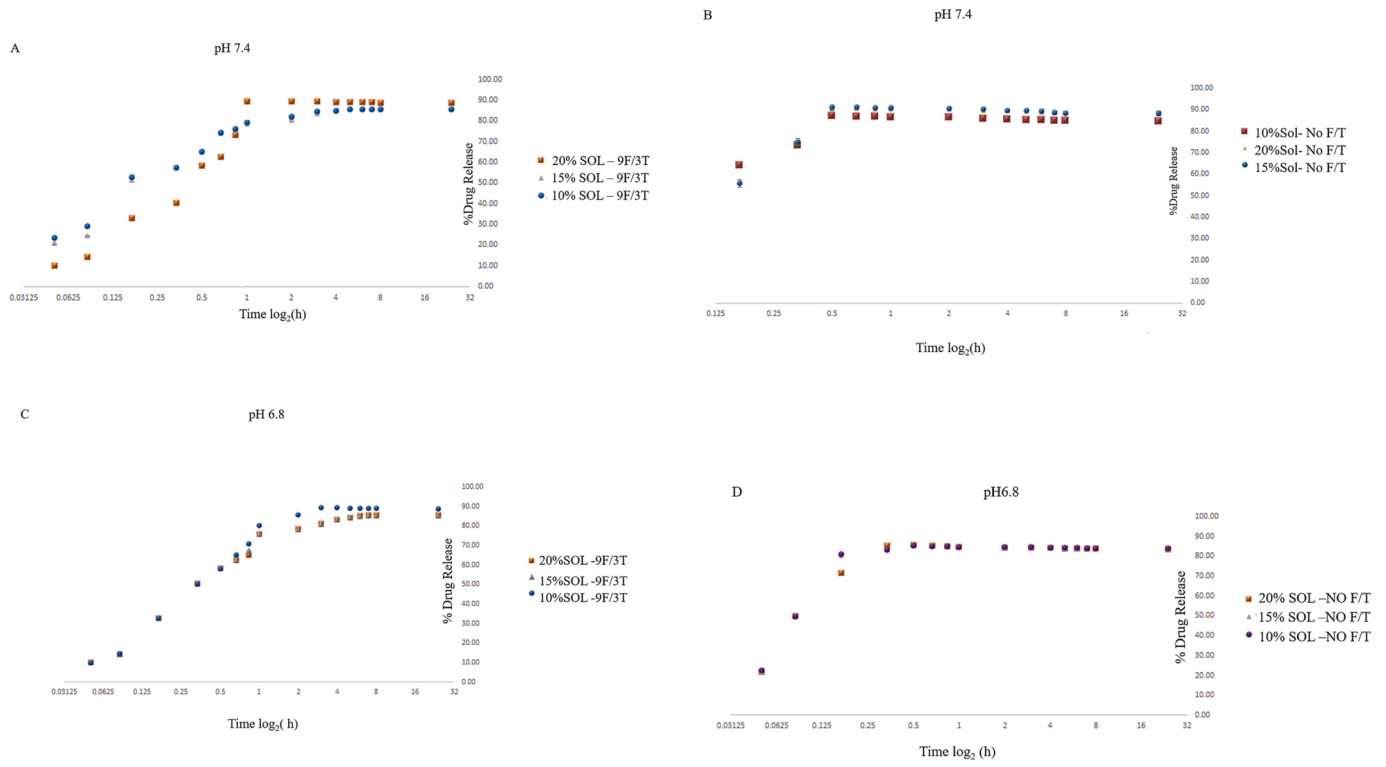

Fig. 7. A) Mean *in vitro* release profiles of RAD001 from the PVA-SOL®-RAD001 NP (N = 3) with 9/3T cycles in pH 7.4 phosphate buffer. B) Mean *in vitro* release profiles of RAD001 from the PVA-SOL®-RAD001 NP (N = 3) with No F/T cycles performed in pH 7.4 phosphate buffer. C) Mean *in vitro* release profiles of RAD001 from the PVA-SOL®-RAD001 NP (N = 3) with 9/3T cycles in pH 6.8 phosphate buffer. D) Mean *in vitro* release profiles of RAD001 from the PVA-SOL®-RAD001 NP (N = 3) with no F/T cycles in pH 6.8 phosphate buffer. Error bars represent standard deviation.

Table 5
A) Model fit parameters for the 2 %PVA-20 %SOL®-RAD001 NP in pH 7.4 buffer within each kinetic model release; B) Model fit parameters for the 2 %PVA-20 % SOL®-RAD001 NP in pH 6.8 buffer within each kinetic model release.

A	F/T Cycles	Zero Order	First Order	Higuchi	Korsmeyer-Peppas		Hixson-Crowell
		R^2	R^2	R^2	R2	n	R^2
	(9F/3T)	−8.4157	0.8531	−3.2096	0.8641	0.345	−1.6518
	No F/T	0.2137	0.966	0.8401	0.9536	0.413	−1.6518
B	F/T Cycles	Zero Order R^2	First Order R^2	Higuchi R^2	Korsmeyer-Peppas R^2	n	Hixson-Crowell R^2
	(9F/3T)	−2.1283	0.8314	−0.0764	0.9583	0.534	−0.3593
	No F/T	−6.0424	0.6859	−2.4019	0.8484	0.534	−3.1727

the RAD-001 release demonstrating that the drug release versus time is linear therefore the release rate is dependent on the drug concentration. For a first order release, the change in concentration with respect to time change is dependent only on concentration. Absorption and elimination of a variety of therapeutic agents has been defined by the first order release kinetics. Based on the release pattern observed, it can be confirmed that a sustained release was achieved for the optimised electro-sprayed PVA-SOL®-RAD001 NP [37]. For pH 6.8 buffer, the Korsmeyer-Peppas was the model of best fit ($R^2 = 9583$ and $R^2 = 0.9660$ respectively) suggesting that the drug release is controlled by a combination of diffusion and erosion. This is further confirmed by the diffusional exponent, n (values $0.43 < n < 0.89$) which describes the mechanism in which the API is released from the matrix. For n values lesser than 0.43, suggests that the release mechanism is governed by diffusion however if the no value is between 0.43 and 0.89 it indicates an anomalous transport mechanism. The n ~ 0.543 value obtained for pH 6.8 suggests that the release is governed by diffusion and swelling, and is time depended following an anomalous (non-fickian) transport mechanism [38].

5. Conclusion

A simple and robust RP-HPLC method was developed and validated using a PDA detector for the quantification of RAD001 in electrosprayed PVA-SOL®-RAD001 NP. The method has been developed in a cost-effective manner owing to the simple mobile phase and the lack of extraction procedures required. The observed results showed that the degradation products formed under different stress conditions of RAD001 did not interfere with the detection of RAD001 and no interference was observed in the chromatogram of the electro-sprayed PVA-SOL®-RAD001 NP. This indicates that the method can be employed for a wide range of drug delivery systems owing to the ability of the method to remain unchanged by small or deliberate variations in method parameters. The need for non-invasive strategies cannot be over-emphasized as currently the go to treatment for any cancerous tumours would be highly invasive surgical resection [39]. In addition, it is important to study the stability of RAD001 under different stress conditions prior to electrospraying, as RAD001 behaves differently under each condition tested. This is cardinal when developing a compatible formulation of drug-polymer–solvent combination to fabricate NP. To the best of our knowledge, the formation of the PVA-SOL®-RAD001 NP via electro-spraying has never been attempted before. The electro-sprayed NP showed efficient encapsulation and a sustained release was achieved in the *in vitro* studies for the freeze-thawed samples compared to the non-freeze-thawed samples owing to the stronger hydrogen bond formation. SOL® is a thermosensitive self-assembling polymer at 37 °C, and the addition of PVA which is a water-soluble

polymer was to ensure the enhancement of drug saturation solubility and mechanical properties, as RAD001 is practically insoluble in water. In comparison to our previously employed sessile droplet technique employed to produce PVA microspheres, electrospraying has a better advantage whereby two different polymers were used to produce more uniform sized particles. The employed ES method further highlights the ability to produce particle size in the nm range, in comparison to our previous study [4]. The use of ES is to control the size and morphology of NP to aid drug delivery across the BBB. Further the ability to blend the two polymers via electrospraying showed improvement in the solubility and mechanical properties as well as the stability of these NP in acidic environments. This not only enhances the mechanical properties of the produced NP but it also helps to sustain the release of RAD001 contributing to anti-tumour efficacy and decreases systemic toxicity. A sustained release would ensure effective concentrations of a drug in the body is achieved, to prevent frequent dosing. Further investigations are required to understand the mechanical properties of the PVA-SOL®-RAD001 via different characterization techniques more in depth in our next article. In conclusion the electro-sprayed PVA-SOL®-RAD001 NP can be applied for a nose-to brain delivery method in the localised treatment of brain tumours to bypass systemic circulation and achieve a sustained release relevant to the current orally available RAD001.

CRediT authorship contribution statement

Lynn Louis: Conceptualization, Methodology, Investigation, Formal analysis, Data curation, Writing – original draft, Writing – review & editing, Visualization. **Bor Shin Chee:** Investigation, Writing – review & editing. **Marion McAfee:** Investigation, Writing – review & editing. **Michael J.D. Nugent:** Supervision, Project administration, Funding acquisition, Conceptualization, Data curation, Formal analysis, Investigation, Methodology, Writing – review & editing.

Declaration of Competing Interest

The authors declare that they have no known competing financial interests or personal relationships that could have appeared to influence the work reported in this paper.

Data availability

Data will be made available on request.

Acknowledgments

This work was supported by the Technological University of the Shannon [President's Doctoral Scholarship].

Appendix A. Supplementary material

Supplementary data to this article can be found online at https://doi.org/10.1016/j.ejpb.2023.09.008.

References

[1] S.S. Prasad, G.V. Krishna Mohan, A. Naga Babu, Development of simple and robust RP-HPLC method for determination of everolimus and its impurities in oral solid dosage form, Asian J. Chem. 31 (2019) 1002–1008, https://doi.org/10.14233/ajchem.2019.21723.
[2] D. Sharmila, Al. Rao, L. Kalyani, Development and validation of stability-indicating high performance liquid chromatographic method for the estimation of everolimus in tablets, Indian J. Pharm. Sci. 77 (2015) 599, https://doi.org/10.4103/0250-474X.169044.
[3] N. Mehra, Mohd. Aqil, Y. Sultana, A grafted copolymer-based nanomicelles for topical ocular delivery of everolimus: Formulation, characterization, ex-vivo permeation, in-vitro ocular toxicity, and stability study, Eur. J. Pharm. Sci. 159 (2021), 105735, https://doi.org/10.1016/j.ejps.2021.105735.
[4] L. Louis, B.S. Chee, N. Louis, G.G. De Lima, M. McAfee, A. Murphy, M.J.D. Nugent, Novel polyvinyl-alcohol microsphere for everolimus delivery for subependymal giant cell astrocytoma, J. Drug Delivery Sci. Technol. 81 (2023), 104204, https://doi.org/10.1016/j.jddst.2023.104204.
[5] B. Melendez, S. Shah, Y. Jiang, J. Dottino, E. Watson, H. Pearce, M. Borthwick, R. E. Schmandt, Q. Zhang, K. Cumpian, J. Celestino, B. Fellman, Y. Yuan, K.H. Lu, A. G. Mikos, M.S. Yates, Novel polymer-based system for intrauterine delivery of everolimus for anti-cancer applications, J. Control. Release 339 (2021) 521–530, https://doi.org/10.1016/j.jconrel.2021.10.008.
[6] G.I. Kirchner, I. Meier-Wiedenbach, M.P. Manns, Clinical pharmacokinetics of everolimus, Clin. Pharmacokinet. 43 (2004) 83–95, https://doi.org/10.2165/00003088-200443020-00002.
[7] A.-N. Sabo, S. Jannier, G. Becker, J.-M. Lessinger, N. Entz-Werlé, V. Kemmel, Sirolimus pharmacokinetics variability points to the relevance of therapeutic drug monitoring in pediatric oncology, Pharmaceutics 13 (2021) 470, https://doi.org/10.3390/pharmaceutics13040470.
[8] D. Krnáč, K. Reiffová, B. Rolinski, A new HPLC-MS/MS method for simultaneous determination of Cyclosporine A, Tacrolimus, Sirolimus and Everolimus for routine therapeutic drug monitoring, J. Chromatogr. B 1128 (2019), 121772, https://doi.org/10.1016/j.jchromb.2019.121772.
[9] B. Felice, M.P. Prabhakaran, M. Zamani, A.P. Rodríguez, S. Ramakrishna, Electrosprayed poly(vinyl alcohol) particles: preparation and evaluation of their drug release profile: Electrosprayed PVA: preparation and evaluation of drug release profile, Polym. Int. 64 (2015) 1722–1732, https://doi.org/10.1002/pi.4972.
[10] S. Zhao, C. Huang, X. Yue, X. Li, P. Zhou, A. Wu, C. Chen, Y. Qu, C. Zhang, Application advance of electrosprayed micro/nanoparticles based on natural or synthetic polymers for drug delivery system, Mater. Des. 220 (2022), 110850, https://doi.org/10.1016/j.matdes.2022.110850.
[11] S. Thakkar, M. Misra, Electrospray drying of docetaxel nanosuspension: A study on particle formation and evaluation of nanocrystals thereof, J. Drug Delivery Sci. Technol. 60 (2020), 102009, https://doi.org/10.1016/j.jddst.2020.102009.
[12] E. Gomaa, M.S. Attia, F.-E.-S. Ghazy, A.E.A. Hassan, A.A. Hasan, Pump-free electrospraying: A novel approach for fabricating Soluplus®-based solid dispersion nanoparticles, J. Drug Delivery Sci. Technol. 67 (2022), 103027, https://doi.org/10.1016/j.jddst.2021.103027.
[13] R.N. Shamma, M. Basha, Soluplus®: A novel polymeric solubilizer for optimization of Carvedilol solid dispersions: Formulation design and effect of method of preparation, Powder Technol. 237 (2013) 406–414, https://doi.org/10.1016/j.powtec.2012.12.038.
[14] D.D. Sun, P.I. Lee, Evolution of supersaturation of amorphous pharmaceuticals: the effect of rate of supersaturation generation, Mol. Pharm. 10 (2013) 4330–4346, https://doi.org/10.1021/mp400439q.
[15] J.D. Wessler, L.T. Grip, J. Mendell, R.P. Giugliano, The P-glycoprotein transport system and cardiovascular drugs, J. Am. Coll. Cardiol. 61 (2013) 2495–2502, https://doi.org/10.1016/j.jacc.2013.02.058.
[16] P. Zi, C. Zhang, C. Ju, Z. Su, Y. Bao, J. Gao, J. Sun, J. Lu, C. Zhang, Solubility and bioavailability enhancement study of lopinavir solid dispersion matrixed with a polymeric surfactant - Soluplus, Eur. J. Pharm. Sci. 134 (2019) 233–245, https://doi.org/10.1016/j.ejps.2019.04.022.
[17] X. Jin, B. Zhou, L. Xue, W. San, Soluplus® micelles as a potential drug delivery system for reversal of resistant tumor, Biomed. Pharmacother. 69 (2015) 388–395, https://doi.org/10.1016/j.biopha.2014.12.028.
[18] H. Adelnia, R. Ensandoost, S. Shebbrin Moonshi, J.N. Gavgani, E.I. Vasafi, H.T. Ta, Freeze/thawed polyvinyl alcohol hydrogels: Present, past and future, Eur. Polym. J. 164 (2022), 110974, https://doi.org/10.1016/j.eurpolymj.2021.110974.
[19] S. Kari, Rapid and Sensitive HPLC Method for Quantification of Everolimus and Its Application in Release Kinetics of Everolimus Eluting Coronary Stents, 2013, 5.
[20] Q 2 (R1) Validation of Analytical Procedures: Text and Methodology, 2006, 15.
[21] F.N. Bonifacio, M. Giocanti, J.P. Reynier, B. Lacarelle, A. Nicolay, Development and validation of HPLC method for the determination of Cyclosporin A and its impurities in Neoral® capsules and its generic versions, J. Pharm. Biomed. Anal. 49 (2009) 540–546, https://doi.org/10.1016/j.jpba.2008.11.027.
[22] N.A. Peppas, E.W. Merrill, Differential scanning calorimetry of crystallized PVA hydrogels, J. Appl. Polym. Sci. 20 (1976) 1457–1465, https://doi.org/10.1002/app.1976.070200604.
[23] P. Halcrow, G. Datta, J.E. Ohm, M.L. Soliman, X. Chen, J.D. Geiger, Role of endolysosomes and pH in the pathogenesis and treatment of glioblastoma, Cancer Reports. 2 (2019), https://doi.org/10.1002/cnr2.1177.
[24] B. Lin, H. Chen, D. Liang, W. Lin, X. Qi, H. Liu, X. Deng, Acidic pH and High-H $_{2}$ O 2 dual tumor microenvironment-responsive nanocatalytic graphene oxide for cancer selective therapy and recognition, ACS Appl. Mater. Interfaces 11 (2019) 11157–11166, https://doi.org/10.1021/acsami.8b22487.
[25] A. Paola, E. Tonhi, P. Silv, Stability Indicating Methods, in: Y. Shoyama (Ed.), Quality Control of Herbal Medicines and Related Areas, InTech, 2011, https://doi.org/10.5772/19940.
[26] V. Vatanpour, B. Kose-Mutlu, I. Koyuncu, Electrospraying technique in fabrication of separation membranes: A review, Desalination 533 (2022), 115765, https://doi.org/10.1016/j.desal.2022.115765.
[27] H. Mateos, L. Gentile, S. Murgia, G. Colafemmina, M. Collu, J. Smets, G. Palazzo, Understanding the self-assembly of the polymeric drug solubilizer Soluplus®, J. Colloid Interface Sci. 611 (2022) 224–234, https://doi.org/10.1016/j.jcis.2021.12.016.
[28] H. Wu, K. Wang, H. Wang, F. Chen, W. Huang, Y. Chen, J. Chen, J. Tao, X. Wen, S. Xiong, Novel self-assembled tacrolimus nanoparticles cross-linking thermosensitive hydrogels for local rheumatoid arthritis therapy, Colloids Surf. B Biointerfaces 149 (2017) 97–104, https://doi.org/10.1016/j.colsurfb.2016.10.013.

[29] C. Sofroniou, M. Baglioni, M. Mamusa, C. Resta, J. Doutch, J. Smets, P. Baglioni, Self-assembly of Soluplus in aqueous solutions: characterization and prospectives on perfume encapsulation, ACS Appl. Mater. Interfaces 14 (2022) 14791–14804, https://doi.org/10.1021/acsami.2c01087.
[30] A.S. Van Dyke, D. Collard, M.M. Derby, A.R. Betz, Droplet coalescence and freezing on hydrophilic, hydrophobic, and biphilic surfaces, Appl. Phys. Lett. 107 (2015), 141602, https://doi.org/10.1063/1.4932050.
[31] A. Bo, T. Kraus, N. De Jonge, Temperature-dependent coalescence of individual nonpolar gold nanoparticles in liquid, ACS Appl. Nano Mater. 6 (2023) 1146–1152, https://doi.org/10.1021/acsanm.2c03818.
[32] B.S. Chee, G.G. de Lima, T.A.M. de Lima, V. Seba, C. Lemarquis, B.L. Pereira, M. Bandeira, Z. Cao, M. Nugent, Effect of thermal annealing on a bilayer polyvinyl alcohol/polyacrylic acid electrospun hydrogel nanofibres loaded with doxorubicin and clarithromycin for a synergism effect against osteosarcoma cells, Mater. Today Chem. 22 (2021), 100549, https://doi.org/10.1016/j.mtchem.2021.100549.
[33] Hydrogels, Cross linking, Gel, Polymer, American Journal of Polymer Science, 2014.
[34] A. Anemone, L. Consolino, L. Conti, P. Irrera, M.Y. Hsu, D. Villano, W. Dastrù, P. E. Porporato, F. Cavallo, D.L. Longo, Tumour acidosis evaluated in vivo by MRI-CEST pH imaging reveals breast cancer metastatic potential, Br. J. Cancer 124 (2021) 207–216, https://doi.org/10.1038/s41416-020-01173-0.
[35] X. Zhang, Y. Lin, R.J. Gillies, Tumor pH and Its Measurement, J. Nucl. Med. 51 (2010) 1167–1170, https://doi.org/10.2967/jnumed.109.068981.
[36] V. Junnuthula, P. Kolimi, D. Nyavanandi, S. Sampathi, L.K. Vora, S. Dyawanapelly, Polymeric micelles for breast cancer therapy: Recent updates, Clin. Transl. Regul. Consider. Pharma. 14 (2022) 1860, https://doi.org/10.3390/pharmaceutics14091860.
[37] A. FDA/CDER/"Yeaton, Dissolution testing and acceptance criteria for immediate-release solid oral dosage form drug products containing high solubility drug substances guidance for industry, 2018.
[38] J.M. Unagolla, A.C. Jayasuriya, Drug transport mechanisms and in vitro release kinetics of vancomycin encapsulated chitosan-alginate polyelectrolyte microparticles as a controlled drug delivery system, Eur. J. Pharm. Sci. 114 (2018) 199–209, https://doi.org/10.1016/j.ejps.2017.12.012.
[39] Y. Feng, Z. Zhang, W. Tang, Y. Dai, Gel/hydrogel-based in situ biomaterial platforms for cancer postoperative treatment and recovery, Exploration 6 (2023) 20220173, https://doi.org/10.1002/EXP.20220173.